

Detection of OH absorption against PSR B1718-35

Anthony H. Minter

National Radio Astronomy Observatory, Green Bank, WV, 24944

tminter@nrao.edu

ABSTRACT

OH absorption against PSR B1718-35 at $(l, b) = 351^{\circ}688, +0^{\circ}671$ has been discovered at 1665 and 1667 MHz using the Green Bank Telescope. The absorption appears to arise at the interface of an H II region and a molecular cloud which are likely associated with the high mass star forming region NGC 6334. Beam dilution is found to be the cause of differences in the opacity of the OH against the Galactic background continuum emission and against the pulsar. The OH cloud is approximately 3 by 1.3 pc and is located behind the H II region.

Subject headings: ISM: clouds — pulsars: individual (PSR B1718-35) — radio lines: ISM

1. Introduction

H I absorption measurements against pulsars have provided a wealth of information on the structure of the Interstellar Medium (ISM). They provide one of the best means of obtaining distance estimates to a large number of pulsars (e.g. Frail & Weisberg 1990). Combining the distances with the pulsar’s dispersion measure (DM) allows the average electron density along the line of sight to the pulsar to be determined. This also allows models of the Galactic electron density to be computed (e.g. Cordes & Lazio 2002, 2003). The H I absorption measurements essentially provide the means by which the electron density model and the atomic neutral gas models of the Galaxy are tied together. Comparison of the H I emission when the pulsar is “off” with the H I absorption against the pulsar can provide information on the density and spin temperature of the absorbing H I gas (e.g. Minter et al. 2005). H I absorption measurements against pulsars have been used to search for structure in the neutral atomic gas on very small scales (e.g. Minter et al. 2005; Weisberg & Stanimirovic 2007). These measurements also play an important role in the study of pulsar population statistics, providing the spatial distribution of pulsars throughout the galaxy (e.g. Lorimer et al. 2006).

It is only natural to attempt to extend absorption measurements against pulsars to molecular gas. Since pulsars have steep spectral indices, it is necessary to look for molecules which have transitions at lower frequencies and which have relatively strong line strengths. This makes the ${}^2\pi_{3/2}(\mathbf{J} = \mathbf{3}/2)$ transitions of the hydroxyl radical (OH) at 1612, 1665, 1667 and 1720 MHz ideal for looking for absorption from molecular material against pulsars.

Previously, only two pulsars have been found which have measurable OH absorption, PSR B1849+00 discovered by Stanimirović et al. (2003) using the Arecibo radio telescope and PSR B1641-45 discovered by Weisberg et al. (2005) using Parkes radio telescope. Both Stanimirović et al. (2003) and Weisberg et al. (2005) observed numerous bright pulsars, 25 in total. In both cases, the OH absorption seen toward the pulsars have unique properties. The OH absorption against the pulsars have narrower linewidths and deeper absorption (larger opacities) than is observed when the pulsar is “off.” This has been attributed to the presence of small scale structure in the molecular material along the lines of sight to the pulsars.

There are a large number of pulsars which have not been observed for OH absorption. In this paper I present observations of sixteen pulsars (PSR B1736-31, PSR B1750-24, PSR B1809-176, PSR B1815-14, PSR B1817-13, PSR B0458+46, PSR B1703-40, PSR B1737-30, PSR B1818-04, PSR B1829-08, PSR B1834-10, PSR B1845-01, PSR B2106+44, PSR B2111+46, PSR B1648-42, and PSR B1718-35) looking for OH absorption. OH absorption was only detected against PSR B1718-35.

2. Observations and Data Reduction

The OH absorption measurements were made using the National Radio Astronomy Observatory’s (NRAO¹) 100 m Green Bank Telescope (GBT). The GBT has an unblocked aperture and a spatial resolution of 7.4 arc-minutes at 1665 MHz. The 1 to 2 GHz receiver, placed at the focus of the Gregorian optics system, was used for the observations. This receiver has a nominal bandpass of 1100–1752 MHz, dual linear polarization and had a system temperature on cold sky of 18 K. The NRAO spectral processor, an FFT spectrometer, was used to simultaneously observe the 1612, 1665, 1667 and 1720 MHz transitions of OH using orthogonal linear polarizations. The spectral processor integration time was approximately 10 seconds, set to the nearest integer number of pulse periods. The spectral processor’s 32-level sampling provides excellent dynamic range when Radio Frequency Interference (RFI)

¹The National Radio Astronomy Observatory is a facility of the National Science Foundation operated under cooperative agreement by Associated Universities, Inc.

is present. Most observations used 256 spectral channels per linear polarization per OH transition with a bandwidth of 2.5 MHz, producing a spectral resolution of $\sim 1.75 \text{ km s}^{-1}$ per channel. Higher resolution observations were performed for PSR B1718-35, using 256 spectral channels per linear polarization per OH transition with a bandwidth of 0.625 MHz, producing a spectral resolution of $\sim 0.44 \text{ km s}^{-1}$ per channel.

The dates and times of the observations are listed in Tables 1 and 2. Table 1 lists the observing dates and times for those pulsars for which OH absorption was not detected. Table 2 lists the dates, times and bandwidths used for the OH absorption observations toward PSR B1718-35. The pulsar OH absorption data were reduced using the technique outlined in Minter et al. (2007). The data were flagged for instances when RFI was present.

PSR B1718-35’s Galactic coordinates are $(l, b) = 351^{\circ}688, +0^{\circ}671$. Since PSR B1718-35 lies in the Galactic plane where continuum emission is present, a slice at constant Galactic longitude was observed at the longitude of PSR B1718-35. The observations went approximately $\pm 5^{\circ}$ out of the galactic plane. These observations allow the Galactic continuum along with the continuum from a discrete object in front of PSR B1718-35 to be measured. Combined with the pulsar “off” spectra, the opacities of the OH lines can then be calculated. The data were corrected for the opacity difference between the zenith and the low elevation ($10^{\circ} - 12^{\circ}$) of the observations. A zenith opacity of $\tau = 0.0103$ at 1666 MHz was used along with an atmospheric temperature of 250 K. The system temperature of ~ 15 K found near the zenith was then subtracted from the data. The remaining brightness temperature was assumed to represent the continuum emission from the Galactic Synchrotron and free-free emission (assumed to be a smooth component) and H II regions or SNRs along the line of sight toward PSR B1718-35.

3. Source Selection

The two prior large searches for OH absorption against pulsars by Stanimirović et al. (2003); Weisberg et al. (2005) selected their targets based on the brightness of the pulsars. This yielded a detection rate of two out of twenty-five (8%). This motivated me to look for a better selection criteria for pulsars with OH absorption.

3.1. Scattering As A Possible Selection Criterion

Boldyrev & Königl (2006) proposed that the strongest Interstellar Scattering (ISS) of pulsar signals was not induced by Kolmogorov-like turbulence in the electrons within the

ISM, but by refraction at the random interface between ionized and non-ionized gas along the line of sight. Particularly, it was predicted that the Photo-Dissociation Regions (PDRs) at the edges of molecular clouds should produce the strongest scattering. Boldyrev & Königl (2006) also suggest that a pulsar’s time broadening would scale as density to the fourth power, ($\tau \propto n^4$), so that only the most dense PDR along the line of sight will dominate the ISS. This will give the appearance of a single scattering screen toward the pulsar which is consistent with what is observed (e.g. Hill et al. 2005).

I list prior attempts to observe OH absorption against pulsars in Table 3. From Table 3 it is seen that the only OH absorption found (including all possible detections) are along lines of sight that are highly scattered and which have large amounts of CO. The pulsars with non-detections are typically bright pulsars, have relatively weak scattering and little CO along their lines of sight. By just looking at bright pulsars, the searches for OH absorption have been biased to lines of sight with little molecular material. If Boldyrev & Königl’s hypothesis is correct then the OH absorption searches have also been biased since they tend to be toward weakly scattered pulsars.

I thus created a list of the most highly scattered pulsars that had a measurable amount of CO along their lines of sight. I obtained the scattering values from the ATNF pulsar catalog (Manchester et al. 2005) and the CO information from Dame et al. (1987). I then selected the pulsars that were outside the Declination range of Arecibo, viewable with the GBT and which could reach a limiting OH opacity of $\tau \sim 0.1$ in less than ten hours as my source list. This list included the pulsars PSR B1736-31, PSR B1750-24, PSR B1809-176, PSR B1815-14, PSR B1817-13 and PSR B1718-35 which were observed in June – October, 2005.

3.2. OH Emission As A Selection Criterion

Another approach that I took was to come up with a list of pulsars that had detectable CO emission along their lines of sight. I excluded pulsars in the declination range of Arecibo, pulsars with Galactic latitudes greater than five degrees, pulsars that would take more than 30 hours to reach $\tau \sim 0.1$ and pulsars that had been previously observed for OH absorption. There were 85 pulsars that met this criteria. I then observed the OH emission toward these pulsars with the GBT to determine which lines of sight had detectable OH (these results will be presented in a future paper; Minter 2008).

OH was detected on the lines of sight toward 34 of the 85 pulsars. The velocity of the OH emission, along with the DM-derived distance of each pulsar, was used to determine which

pulsars could have OH between the Sun and the pulsar. This then led to observations of PSR B0458+46, PSR B1703-40, PSR B1737-30, PSR B1818-04, PSR B1829-08, PSR B1834-10, PSR B1845-01, PSR B2106+44, PSR B2111+46 and PSR B1648-42 with the GBT to search for OH absorption against these pulsars.

4. Results

No OH absorption was detected toward PSR B1736-31, PSR B1750-24, PSR B1809-176, PSR B1815-14, PSR B1817-13, PSR B0458+46, PSR B1703-40, PSR B1737-30, PSR B1818-04, PSR B1829-08, PSR B1834-10, PSR B1845-01, PSR B2106+44, PSR B2111+46, and PSR B1648-42. The 1σ upper limits for the opacity for OH absorption toward these pulsars is shown in Table 4. PSR B1750-24 did not have any detectable OH in the pulsar “off” spectra and was thus not observed for a significant amount of time, resulting in its higher opacity limit. OH absorption was only detected against PSR B1718-35.

4.1. PSR B1718-35 OH Absorption Properties

I show the OH absorption spectra against PSR B1718-35 as well as the pulsar “off” OH spectra for the two resolution modes (1.75 and 0.44 km s^{-1}) in Figures 1 and 2. After initially detecting the OH absorption against PSR B1718-35 in the lower resolution mode, which allowed a large velocity range to be searched, I switched to the higher resolution mode to resolve the narrow absorption lines that were present. The results of Gaussian fits to the OH absorption lines are presented in Table 5. As can be seen from the results in Table 5, the initial wide-bandwidth observations, which had a spectral resolution slightly larger than the true linewidths of the spectral lines, are clearly affected by poor spectral resolution.

4.1.1. Column Density of the OH Absorbing Cloud

From the observed opacity of the 1667 MHz absorption against PSR B1718-35, we can estimate the OH column density, N_{OH} , in the absorbing cloud. Using equation 9.12 of Elitzur (1992), along with $\tau(1667) = 0.3 \pm 0.003$ and a linewidth of $\Delta v = -1.5 \pm 0.2$, the OH column density is given by

$$N_{OH} = \frac{1. \pm 0.1 \times 10^{14}}{T_x(1667)} \text{ cm}^{-2} \quad (1)$$

where $T_x(1667)$ is the excitation temperature of the line which is typically 5-10 K (Elitzur 1992). The observed linewidth limits the thermal temperature of the OH to be $T < 830 \pm 240$ K, resulting in the limit that $N_{OH} > 1.2 \pm 0.1 \times 10^{11} \text{ cm}^{-2}$. From the typical excitation temperatures, the likely column density is of the order $N_{OH} \sim 10^{13} \text{ cm}^{-2}$. For OH column densities between $10^{14} < \frac{N_{OH}}{\Delta v} < 10^{15} \text{ cm}^{-2} \text{ s km}^{-1}$ the satellite lines at 1612 and 1720 MHz are conjugates with the 1720 MHz line being in emission and the 1612 MHz line being in absorption (Weisberg et al. 2005). At column densities $\frac{N_{OH}}{\Delta v} > 10^{15} \text{ cm}^{-2} \text{ s km}^{-1}$ the lines remain conjugates but with the 1612 MHz line being in emission and the 1720 MHz line being in absorption. Both of these cases occur when the region containing the OH is optically thick to infra-red photons. As can be seen in the pulsar “off” spectra in Figure 2, the 1612 MHz line is in emission at the velocity where absorption is seen against the pulsar. However, the 1720 MHz line is not detected at a 3σ limit of 0.08 K. This is significantly less than the -0.25 K that we would expect if the 1720 MHz line exhibited conjugate emission with the 1612 MHz line. This indicates that the OH column density is $N_{OH} < 6.7 \pm 0.9 \times 10^{13} \text{ cm}^{-2}$ in the OH absorption absorbing cloud toward PSR B1718-35. Using the standard abundance ratio of $N_{OH}/N_H = 6 \times 10^{-8}$ (Elitzur 1992), the total hydrogen column density in the absorbing cloud is of the order $N_H \sim (1.7 - 11.1) \times 10^{20} \text{ cm}^{-2}$. The H I absorption against PSR B1718-35 was measured by Weisberg et al. (1995) and is shown in their Figure 1d. At the velocity of the OH absorption, the H I absorption has an opacity $\tau > 2$ and the emission has $T_B \sim 100$ K. Assuming that half of the total H I emission comes from the same side of the tangent point² as the OH cloud results in an estimated column density $N_{HI} > 1.8 \times 10^{20} \text{ cm}^{-2}$ which is consistent with the column density derived from OH.

4.1.2. The Distance To The OH Cloud

Weisberg et al. (1995) determined that the H I kinematic distance to PSR B1718-35 is 5.6 ± 0.6 kpc. This puts PSR B1718-35 on the near side of the tangent point for its line of sight. The Galactic bar is on the far side of the tangent point for the PSR B1718-35 line of sight and can be ignored in the following discussions.

I show the velocity–distance relationship for the PSR B1718-35 line of sight using the flat rotation curve of Fich et al. (1989) In Figure 3. In determining the distance of the OH cloud from its velocity, a random motion for cold clouds of 7 km s^{-1} has been used

²The velocity–distance relationship is doubled valued for the PSR B1718-35 line of sight. Since the Galactic latitude is small, $b = 0^\circ 671$, we can expect that the line of sight we encounter equal amounts of gas on the near side and the far side of the tangent point. Thus the total emission at any velocity will have half of its contribution from the near side with the other half coming from the far side of the tangent point.

(Lockman & Dickey 1990). This random velocity was used as an error on the distance model as suggested in Minter et al. (2007). An upper limit of 1.86 kpc is found for the distance to the OH cloud.

The line of sight toward PSR B1718-35 is in the extended halo of radio continuum emission surrounding NGC 6334 (see the Figure on page 347 of Altenhoff et al. 1970). Comparing the observed velocity range, -1.5 to -1.9 km s^{-1} , for the OH absorption against PSR B1718-35 with the CO velocities of Dickel et al. (1977) shows that the OH cloud has the same velocity as NGC 6334 B and the extended CO emission to the north-east of NGC 6334 (see Figure 6 of Dickel et al. 1977). H II regions in and around NGC 6334 have velocities in the range $+1$ to -7 km s^{-1} (Lockman 1989; Quireza et al. 2006). It is thus quite possible that the OH cloud is part of the NGC 6334 Giant Molecular Cloud. If this is the case then we can place the OH cloud at the distance of NGC 6334, 1.7 ± 0.3 kpc (Neckel 1978), which is consistent with the kinematic distance upper limit.

4.2. The Continuum Emission Toward PSR B1718-35

The observed continuum emission in a “slice” at the constant Galactic longitude of PSR B1718-35 ($351^\circ 688$) is shown in Figure 5. The total continuum emission toward PSR B1718-35 in the GBT beam is 9.04 ± 0.05 K. A two component Gaussian fit that can be assumed to approximate the smooth Galactic synchrotron and free-free emission contribution to the continuum emission was made. As can be seen in Figure 5, this approximates the smooth background continuum emission from Galactic synchrotron and free-free emission reasonably well. This fit then sets the smooth Galactic component emission at 5.8 K and the continuum in front of PSR B1718-35 as having 3.51 K. The continuum emission in front of the pulsar comes from three different source that are slightly blended (this is easily seen in Figure 4). At a Galactic latitude lower than PSR B1718-35 is the H II region G351.662+0.518 (Lockman 1989) and at a higher Galactic latitude is the SNR G351.7+0.8 (Green 2006; Whiteoak & Green 1996). Fitting an additional three Gaussians to this emission results in a brightness temperature of 4.1 ± 0.2 K for G351.662+0.518, 4.2 ± 0.2 K for SNR G351.7+0.8 and 2.9 ± 0.2 K for the continuum source in front of PSR B1718-35. Data from the Parkes 6 cm survey of the southern Galactic plane at 5009 MHz (Haynes et al. 1978) shows that the continuum source in front of PSR B1718-35 has a flux of 2.3 ± 0.2 K for the PSR B1718-35 line of sight. This then gives a spectral index of -0.21 ± 0.2 (using $S = \nu^\alpha$) which is consistent with the expected H II region thermal emission spectral index of -0.07 .

4.3. Comparing The Pulsar “On” and “Off” OH Absorption Spectra

For the two previous detections of OH absorption against pulsars, the opacity of the absorption has been greater and the linewidths have been narrower against the pulsar than against the continuum background (see Stanimirović et al. 2003; Weisberg et al. 2005). Two viable explanations were put forward in Stanimirović et al. (2003): a) the absorption comes from OH clouds whose angular size is larger than the observed scattering size of the pulsar but smaller than the angular size of the telescope beam; or b) there are extra OH clouds that are seen in absorption against the continuum background with the larger telescope beam that are not seen along the pulsar line of sight. In the former case, if the OH cloud seen in absorption against the pulsar could be spectroscopically isolated in the pulsar ‘off’ spectrum, then the linewidths in the two spectra should be the same. The differences in the optical depth of the line could then be used to constrain the size of the cloud. In the later case, the OH cloud is expected to be built from smaller “cloudlets” (Stanimirović et al. 2003) and we would expect the linewidths and the opacities to be different between the pulsar absorption and the continuum background absorption spectra. Of course, both of these scenarios could be operating at the same time.

In Figure 2 we see that the 1665 and 1667 MHz absorption lines at $\sim 1.7 \text{ km s}^{-1}$ have a narrow component and a broader component. Gaussian fits for a narrow and broad linewidth components to the 1667 MHz background continuum absorption spectrum are presented in Table 6. The broad component Gaussian fit is shown in the top panel of Figure 6. Comparing the results in Table 6 and Table 5, we see that the narrow component has the same velocity and that the linewidths agree at the 1σ level for the pulsar and continuum background cases. In the bottom panel of Figure 6, I show the opacities of the two narrow components and the difference between them. The opacity of the pulsar “off” spectra was determined using an effective continuum strength of 2.1 K (see below) which makes the opacities equal. As can be seen in Figure 6, there is no discernible difference between the narrow component in the pulsar “off” spectrum and the absorption against the pulsar. Thus, only the size of the OH cloud will play a role in any difference between the opacity observed against the background continuum and against the pulsar.

Since we know the opacity of the OH from the absorption against the pencil-thin beam of the pulsar and there is information on the continuum brightness, limits can be determined for the size of the OH absorption cloud. This is done using

$$e^{-\tau} = \frac{I(\nu)}{f_{\Omega} T_{bg}} + 1 = \frac{I(\nu)}{T_{eff}} + 1 \quad (2)$$

where $I(\nu)$ is the measured, baseline subtracted spectrum (top panel of Figure 6) and $f_{\Omega} = \Omega_{OH}/\Omega_{GBT}$ is the size of the OH cloud (Ω_{OH}) relative to the size of the telescope beam

(Ω_{GBT}). $T_{eff} = f_{\Omega}T_{bg}$ is the effective brightness temperature and corresponds to the OH cloud size weighted background brightness temperature averaged over the entire GBT beam. Performing a least-squares, non-linear fit to the observed narrow linewidth component results in $T_{eff} = 2.1 \pm 0.2$ K. Allowing all of the continuum flux to reside behind the OH cloud, $T_{bg} = 8.7 \pm 0.2$ K where 5.8 K is from the smooth Galactic continuum and 2.9 K is from the H II region, gives a minimum size of the cloud assuming that the cloud is spherically symmetric. For this case $f_{\Omega} = 0.24 \pm 0.02$. Using the 7.4 arc-minute FWHM size of the GBT beam, the minimum OH cloud radius is 0.89 ± 0.08 arc-minutes which at a distance of 1.7 kpc corresponds to 0.44 ± 0.04 pc. If the OH cloud is behind the H II region, and assuming that there is little contribution to the Galactic continuum between the Sun and NGC 6334, $f_{\Omega} = 0.36 \pm 0.04$ and the size of the OH cloud would be 1.3 ± 0.1 arc-minutes, which corresponds to 0.64 ± 0.06 pc at a distance of 1.7 kpc. These size scales along with the column densities derived in § 4.1.1 translate into densities of order $n_H \sim 10 - 100 \text{ cm}^{-3}$ for the OH cloud.

An ellipse with semi-major and semi-minor axes of 3 and 1.8 arc-minutes roughly covers the area of 8 micron emission seen in Figure 4. If we assume that the OH cloud size is represented by the 8 micron dust cloud size, then $f_{\Omega} \sim 0.36$. This is the same number derived above assuming that the OH cloud is behind the H II region and in front of most of the Galactic background continuum emission. It seems likely that the OH cloud lies behind the H II region.

From the FWHM linewidths in Table 6, the narrow linewidth component corresponds to a thermal temperature $T < 830 \pm 240$ K. The broad linewidth component corresponds to a thermal temperature of $T < 10400 \pm 1200$ K. Since the OH might be expected to be in regions with temperatures in the range 10 – 100 K, there is obviously a very large turbulent component to the linewidths. The two components fit in very nicely with the molecular cloud (MC) – H II region interaction scenario. The narrow linewidth OH could be in the part of the MC that has not yet interacted with the H II region while the broad linewidth component is in the part of the MC interacting with the H II region.

4.4. Energy Input Into The Molecular Cloud

If it is assumed that there is an interaction between the MC and an H II region, then we can estimate the amount of energy input into the MC. This is done by comparing the linewidths of the narrow and broad components. From the above size (6 by 2.6 arcminutes or 2.97 by 1.28 pc at a distance of 1.7 kpc) and column density estimates ($N_{OH} < 6.7 \times 10^{13} \text{ cm}^{-2}$), there are $< 2.4 \times 10^{51}$ OH particles in the narrow line component of the cloud. An OH

linewidth of 1.5 km s^{-1} corresponds to an energy of 3.2×10^{-13} ergs for each OH molecule, using $E = 1/2mv^2$. This gives a total energy of $< 7.7 \times 10^{38}$ ergs for all the OH molecules in the narrow linewidth component. An OH linewidth of 5.3 km s^{-1} corresponds to an energy of 4.0×10^{-12} ergs for each OH molecule in the broad linewidth component of the OH cloud. The broad line-component has the same characteristics between the 1720 and 1612 MHz lines as does the narrow linewidth component. We can thus limit the column density of the broad line to be $N_{OH} < 1.9 \times 10^{13} \text{ cm}^{-2}$ which results in a total energy of $< 2.1 \times 10^{39}$ ergs for all the OH molecules in the broad linewidth component. This suggests that a few times 10^{39} ergs of energy have been input into the broad linewidth component.

If we assume that the same amount of energy per particle has been added to all molecular species in the broad component of the OH cloud, then a total of a few times 10^{46} ergs of energy have been deposited into the cloud. SNR typically involve a release of $\sim 10^{51}$ ergs of energy. A cluster of O and B stars that form H II regions can also output $\sim 10^{51}$ ergs of energy over their lifetimes. So it is not unreasonable to assume that the broad linewidth component of the OH cloud has interacted with an H II region or SNR.

5. Conclusions

PSR B1718-35 is only the third pulsar found to have OH absorption. In all three cases the OH absorption arises in the interaction of a MC with a SNR or an H II region. Forty-seven (47) pulsars have been searched for OH absorption. This suggests that OH absorption against pulsars is either quite rare, or that the absorption in most MCs is very weak and below the detection capabilities of current telescopes without very deep searches. That all known cases involve a MC that is in the process of being destroyed by a SNR or H II region and that the detection rate is only $\sim 6\%$ implies that OH absorption against pulsars is a rare occurrence.

The detection rate using pulsar brightness is about $\sim 6\%$. I found a detection rate of 17% using scintillation strength for the selection criteria. I also had a detection rate of 0% using detected OH emission that could be between the Sun and the pulsar. Since the PSR B1718-35 OH detection was found in a search of six pulsars based on their strong scattering, and PSR B1718-35 is the 7th most strongly scattered pulsar, some credence can be given to the hypothesis of Boldyrev & Königl (2006) but it by no means provides conclusive proof for their idea that scattering originates in PDRs at the boundaries of H II regions and MCs.

In all likelihood, the continuum object along the line of sight toward PSR B1718-35 is an H II region associated with the NGC 6334 complex. The spectral index of the source is

consistent with what is expected for an H II region. The morphology (see Figure 4) of cold dust surrounding warm dust is not consistent with the source being a SNR. There is some H_α emission associated with the continuum source (see Figure 4). Unfortunately, the SHASSA survey (Gaustad et al. 2001) does not provide velocity information for the H_α . Although this line of sight was observed as part of the WHAM survey (Haffner et al. 2003), the 1° resolution convolves the emission from the H II region toward PSR B1718-35 with other H II regions in NGC 6334. Thus it is not known if the H_α arises at the same velocities as the OH absorption against PSR B1718-35. Hydrogen radio recombination lines or higher spatial resolution H_α with velocity information observations should be performed to confirm that the continuum source is an H II region.

It was found that the OH cloud along the line of sight of PSR B1718-35 is likely behind the H II region. The OH cloud has a broad linewidth component and a narrow linewidth component. Only the narrow linewidth component is seen in absorption against PSR B1718-35. A similar situation of broad and narrow linewidth components with only the narrow component seen in absorption against the pulsar was observed for PSR B1849+00 (Stanimirović et al. 2003). This is also the case for PSR B1641-45 (Weisberg et al. 2005). The opacities of the OH absorption against PSR B1718-35 and against the continuum background (pulsar “off” spectrum) can be reconciled via consideration of the beam-filling factor of the OH cloud. This should be investigated further for the PSR B1849+00 and PSR B1641-45 OH absorption.

This work is based [in part] on observations made with the Spitzer Space Telescope, which is operated by the Jet Propulsion Laboratory, California Institute of Technology under a contract with NASA. The Southern H-Alpha Sky Survey Atlas (SHASSA) is supported by the National Science Foundation.

REFERENCES

- Altenhoff, W. J., Downes, D., Goad, L., Maxwell, A., & Rinehart, R. 1970, *A&AS*, 1, 319
- Boldyrev, S., & Königl, A. 2006, *ApJ*, 640, 344
- Cordes, J. M., & Lazio, T. J. W. 2002, *ArXiv Astrophysics e-prints*, arXiv:astro-ph/0207156
- Cordes, J. M., & Lazio, T. J. W. 2003, *ArXiv Astrophysics e-prints*, arXiv:astro-ph/0301598
- Dame, T. M., et al. 1987, *ApJ*, 322, 706

- Dickel, H. R., Dickel, J. R., & Wilson, W. J. 1977, *ApJ*, 217, 56
- Elitzur, M. 1992, *Astrophysics and Space Science Library*, 170, p. 234
- Fich, M., Blitz, L., & Stark, A. A. 1989, *ApJ*, 342, 272
- Frail, D. A., & Weisberg, J. M. 1990, *AJ*, 100, 743
- Galt, J. A. 1974, *A&A*, 31, 235
- Gaustad, J. E., McCullough, P. R., Rosing, W., & Van Buren, D. 2001, *PASP*, 113, 1326
- Green D. A., 2006, “A Catalogue of Galactic Supernova Remnants (2006 April version)”, Astrophysics Group, Cavendish Laboratory, Cambridge, United Kingdom (available at <http://www.mrao.cam.ac.uk/surveys/snrs/>)
- Haffner, L. M., Reynolds, R. J., Tufte, S. L., Madsen, G. J., Jaehnig, K. P., & Percival, J. W. 2003, *ApJS*, 149, 405
- Haynes, R. F., Caswell, J. L., & Simons, L. W. J. 1978, *Australian Journal of Physics Astrophysical Supplement*, 45, 1
- Hill, A. S., Stinebring, D. R., Asplund, C. T., Berwick, D. E., Everett, W. B., & Hinkel, N. R. 2005, *ApJ*, 619, L171
- Lockman, F. J., & Dickey, J. M. 1990, *ARAA*, 28, 215
- Lockman, F. J. 1989, *ApJS*, 71, 469
- Lorimer, D. R., et al. 2006, *MNRAS*, 372, 777
- Manchester, R. N., Hobbs, G. B., Teoh, A., & Hobbs, M. 2005, *AJ*, 129, 1993
- Minter, A. H., 2008, in preparation.
- Minter, A. H., Camilo, F., Ransom, S. M., Halpern, J. P., & Zimmerman, N. 2007, *ArXiv e-prints*, 705, arXiv:0705.4403
- Minter, A. H., Balser, D. S., & Kartaltepe, J. S. 2005, *ApJ*, 631, 376
- Neckel, T. 1978, *A&A*, 69, 51
- Quireza, C., Rood, R. T., Balser, D. S., & Bania, T. M. 2006, *ApJS*, 165, 338
- Slysh, V. I. 1972, *Astronomicheskij Tsirkulyar*, 731, 1

Stanimirović, S., Weisberg, J. M., Dickey, J. M., de la Fuente, A., Devine, K., Hedden, A.,
& Anderson, S. B. 2003, *ApJ*, 592, 953

Weisberg, J. M., Siegel, M. H., Frail, D. A., & Johnston, S. 1995, *ApJ*, 447, 204

Weisberg, J. M., Johnston, S., Koribalski, B., & Stanimirović, S. 2005, *Science*, 309, 106

Whiteoak, J. B. Z., & Green, A. J. 1996, *A&AS*, 118, 329

Weisberg, J. M., & Stanimirovic, S. 2007, *ArXiv Astrophysics e-prints*,
arXiv:astro-ph/0701771

Table 1. Dates of the observations for the pulsars without detectable OH absorption with the GBT.

Pulsar	Galactic Coordinates		Dates of Observations	Integration Time (hrs)
	l	b		
PSR B1736-31	357°099	−0°219	2005 Jul 31 – Aug 08	5.5
PSR B1750-24	4°257	+0°503	2005 Aug 25 – Aug 26	4.75
PSR B1809-176	12°909	+0°388	2005 Aug 06 – Aug 25	10.5
PSR B1815-14	16°406	+0°610	2005 Jun 09 – Aug 06	9.25
PSR B1817-13	17°160	+0°482	2005 Jun 01 – Sep 01	18.25
PSR B0458+46	160°363	+3°077	2006 May 14 – Sep 30	36.75
PSR B1703-40	345°718	−0°197	2006 Jun 02 – Aug 29	6.0
PSR B1737-30	358°295	+0°238	2006 Jul 21 – Jul 30	3.75
PSR B1818-04	25°456	+4°732	2006 May 27 – Oct 31	18.75
PSR B1829-08	23°272	+0°298	2006 Jul 21 – Jul 27	10.25
PSR B1834-10	22°263	−1°415	2006 Jun 07 – Jun 29	5.75
PSR B1845-01	31°339	+0°039	2006 May 08	6.0
PSR B2106+44	86°909	−2°012	2006 Jun 19 – Jul 25	8.25
PSR B2111+46	89°003	−1°266	2006 May 15 – May 19	5.25
PSR B1648-42	342°457	+0°922	2006 May 29 – May 31	4.5

Table 2. Dates of observations detecting OH absorption toward PSR B1718-35 with the GBT.

Date	Bandwidth Per Band (MHz)
2005 Aug. 24–29	2.5
2005 Aug. 29–31	0.625
2005 Oct. 08	0.625

Table 3. Results of previous searches for OH absorption against pulsars. The first column gives the pulsar observed. The second column is the pulse broadening time found in the ATNF pulsar catalog (Manchester et al. 2005) while the third column gives the ranking in terms of the strength of the pulse broadening for all pulsars. The fourth column gives the integrated CO intensity for all CO along the line of sight (not necessarily just the CO that is foreground to the pulsar) using the survey data from Dame et al. (1987). The fifth column gives the observed opacity or opacity limits where mentioned. The sixth column gives the reference for the OH absorption observations.

Pulsar	$\tau_{\text{sc}}^{1\text{GHz}}$ (sec)	τ_{sc} Rank	W_{CO} (K km sec $^{-1}$)	<i>Opacity</i>	Reference
PSR B1849+00	1.51×10^{-1}	4	121.58	0.9	Stanimirović et al. (2003)
PSR B1737+13	9.33×10^{-8}	106	–	–	Stanimirović et al. (2003)
PSR B1933+16	1.51×10^{-5}	71	–	–	Stanimirović et al. (2003)
PSR B2016+28	3.89×10^{-8}	115	0.37	–	Stanimirović et al. (2003)
PSR B1944+17	4.27×10^{-8}	114	0.05	–	Stanimirović et al. (2003)
PSR B1915+13	3.47×10^{-5}	65	90.86	possible	Stanimirović et al. (2003)
PSR B1929+10	1.78×10^{-9}	142	0.03	–	Stanimirović et al. (2003)
PSR B1641-45	1.12×10^{-2}	29	133.25	0.1	Weisberg et al. (2005)
PSR B0740-28	7.76×10^{-6}	76	6.06	< 0.1	Weisberg et al. (2005)
PSR B0833-45	6.03×10^{-5}	62	0.00	< 0.1	Weisberg et al. (2005)
PSR B0835-41	7.59×10^{-6}	77	2.11	< 0.07	Weisberg et al. (2005)
PSR B0906-49	–	–	–	< 0.1	Weisberg et al. (2005)
PSR B1054-62	–	–	–	< 0.1	Weisberg et al. (2005)
PSR B1055-52	–	–	–	< 0.1	Weisberg et al. (2005)
PSR B1154-62	–	–	–	< 0.3	Weisberg et al. (2005)
PSR B1240-64	–	–	–	< 0.1	Weisberg et al. (2005)
PSR B1323-58	2.88×10^{-3}	44	1.02	< 0.1	Weisberg et al. (2005)
PSR B1323-62	7.76×10^{-6}	76	6.06	< 0.1	Weisberg et al. (2005)
PSR B1557-50	4.47×10^{-3}	39	16.81	< 0.1	Weisberg et al. (2005)
PSR B1601-52	–	–	–	< 0.2	Weisberg et al. (2005)
PSR B1742-30	–	–	–	< 0.2	Weisberg et al. (2005)
PSR B1749-28	5.50×10^{-7}	88	55.67	< 0.05	Weisberg et al. (2005)
PSR B1800-31	–	–	–	< 0.3	Weisberg et al. (2005)
PSR B1822-09	2.19×10^{-7}	96	9.89	< 0.3	Weisberg et al. (2005)
PSR B1826-17	–	–	–	< 0.3	Weisberg et al. (2005)
PSR B0329+54	6.31×10^{-8}	111	0.08	< 0.1	Galt (1974)
PSR B0450+55	2.57×10^{-8}	121	0.34	< 0.04	Slysh (1972)
PSR B0525+21	2.88×10^{-7}	92	–	< 0.15	Slysh (1972)
PSR B0740-28	7.76×10^{-6}	76	6.06	–	Slysh (1972)
PSR B1642-03	6.76×10^{-8}	109	–	–	Slysh (1972)

Table 4. 1σ Opacity upper limits for OH absorption toward the pulsar observations presented in this paper. Note that the GBT L-band receiver has a resonance around 1720 MHz which causes the sensitivity at this frequency to be compromised, as one polarization does not contribute very much to the signal-to-noise.

Pulsar	Opacity Upper Limits			
	1665 MHz	1667 MHz	1612 MHz	1720 MHz
PSR B1736-31	0.07	0.06	0.08	0.1
PSR B1750-24	0.2	0.2	0.2	0.4
PSR B1809-176	0.06	0.06	0.06	0.10
PSR B1815-14	0.03	0.03	0.03	0.04
PSR B1817-13	0.04	0.05	0.04	0.09
PSR B0458+46	0.06	0.06	0.06	0.07
PSR B1703-40	0.07	0.08	0.07	0.1
PSR B1737-30	0.1	0.1	0.1	0.1
PSR B1818-04	0.05	0.05	0.04	0.04
PSR B1829-08	0.2	0.2	0.2	0.7
PSR B1834-10	0.08	0.08	0.07	0.09
PSR B1845-01	0.04	0.04	0.03	0.07
PSR B2106+44	0.09	0.1	0.1	0.1
PSR B2111+46	0.04	0.04	0.04	0.05
PSR B1648-42	0.06	0.06	0.05	0.07

Table 5. Gaussian fit results for the observed OH absorption against PSR B1718-35.

ν (MHz)	$\Delta\nu$ (MHz)	σ_τ	τ	V_{lsr} (km s ⁻¹)	FWHM (km s ⁻¹)
1665	2.5	0.008	0.076 ± 0.009	-1.5 ± 0.2	3.0 ± 0.4
1667	2.5	0.009	0.074 ± 0.008	-2.0 ± 0.2	3.2 ± 0.4
1612	2.5	0.01	0.042 ± 0.009	-1.3 ± 0.4	3 ± 1
1720	2.5	0.01
1665	0.625	0.04	0.20 ± 0.03	-1.6 ± 0.1	1.6 ± 0.3
1667	0.625	0.04	0.30 ± 0.03	-1.86 ± 0.07	1.5 ± 0.2
1612	0.625	0.04	0.14 ± 0.03	-1.7 ± 0.1	1.5 ± 0.4
1720	0.625	0.06

Table 6. Gaussian fit results for the observed 1667 MHz OH absorption against the background continuum emission (pulsar “off” spectrum). The opacities were determined using an effective background continuum emission of 2.1 K.

τ	V_{lsr} (km s^{-1})	FWHM (km s^{-1})
0.30 ± 0.02	-1.86 ± 0.03	1.8 ± 0.1
0.23 ± 0.02	-1.91 ± 0.07	5.3 ± 0.3

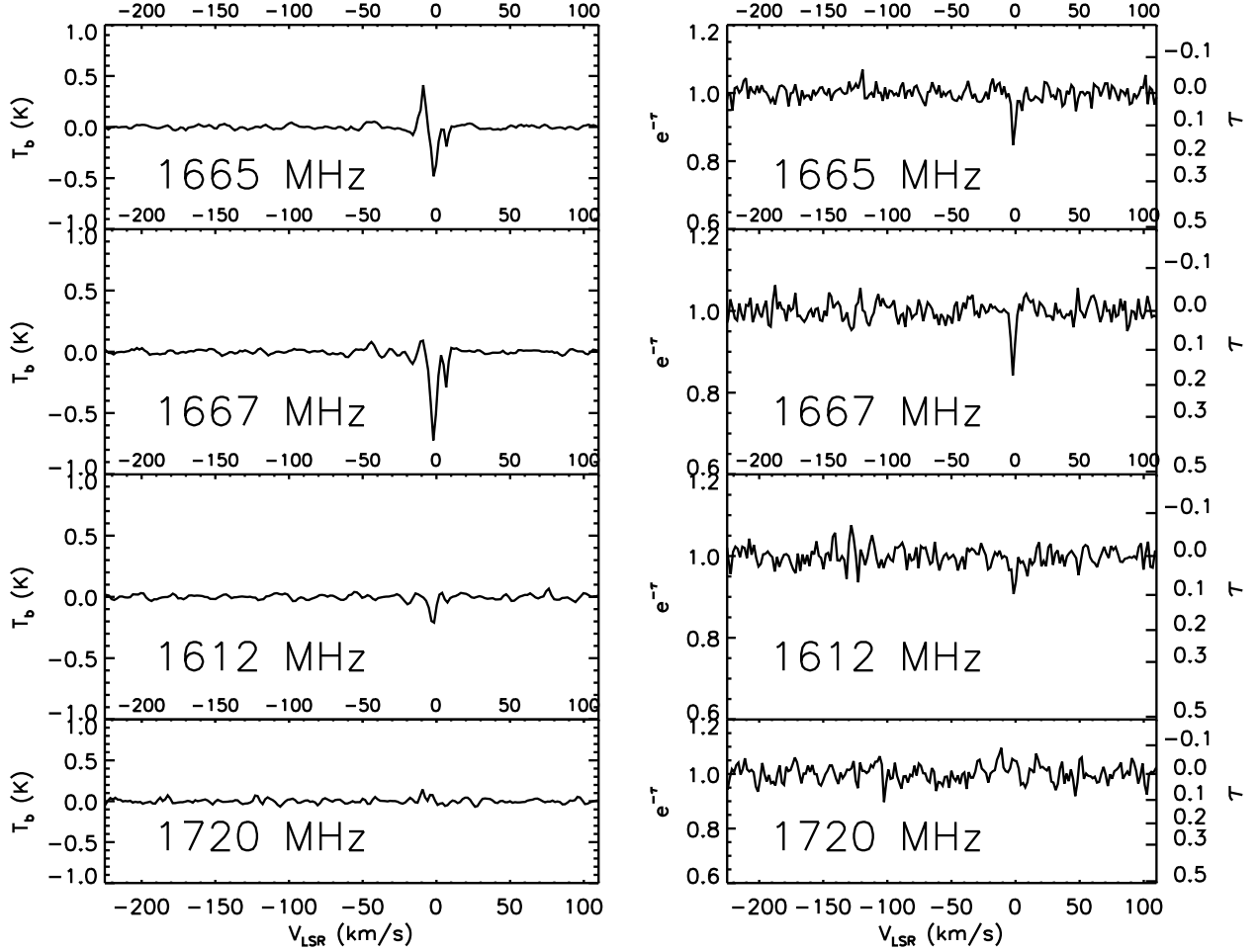


Fig. 1.— The observed OH opacities observed against PSR B1718-35 with 1.75 km s^{-1} spectral resolution. The left column shows the pulsar “off” spectra and the right column shows the OH absorption against PSR B1718-35.

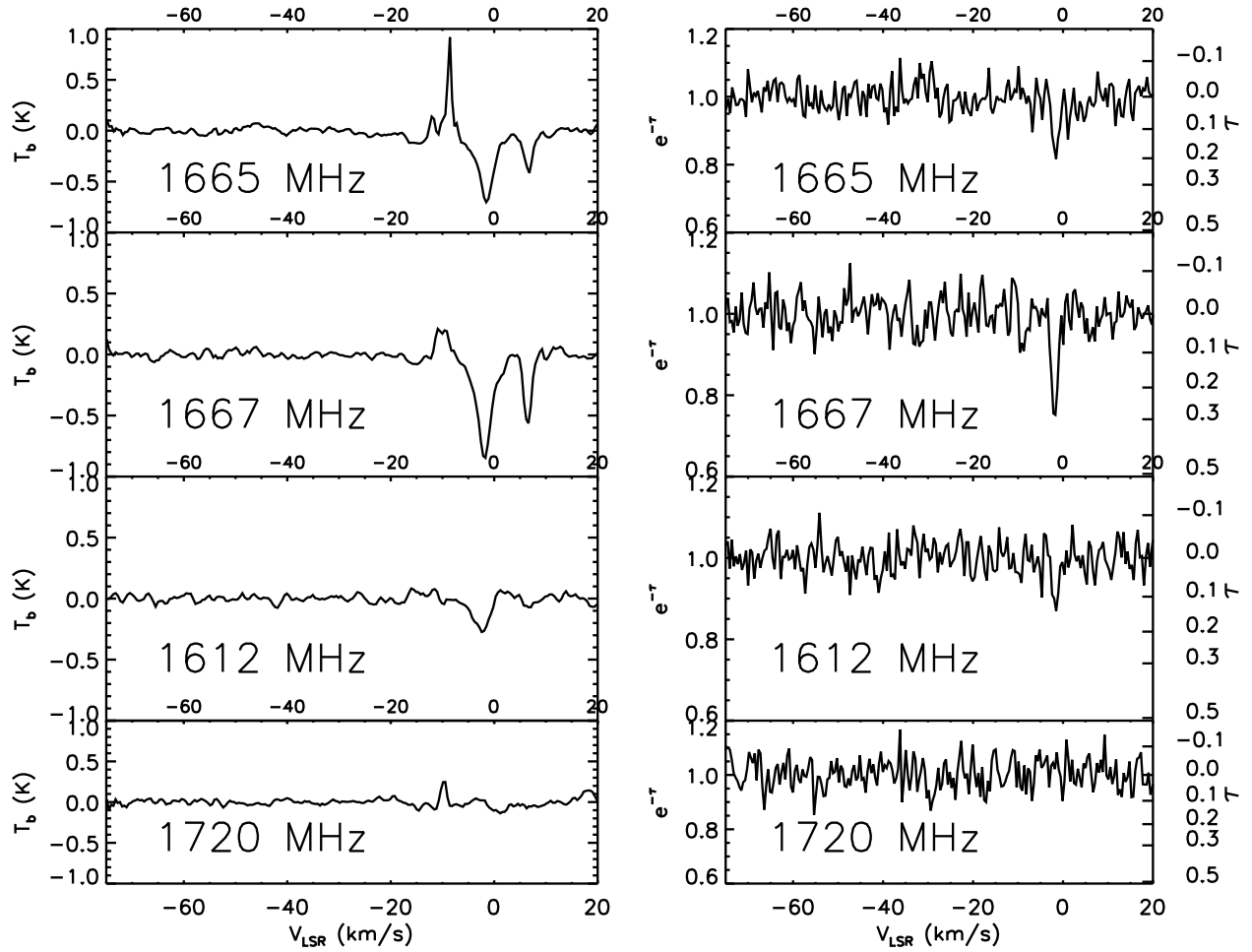


Fig. 2.— The same as Figure 1 except for the higher 0.44 km s^{-1} spectral resolution data.

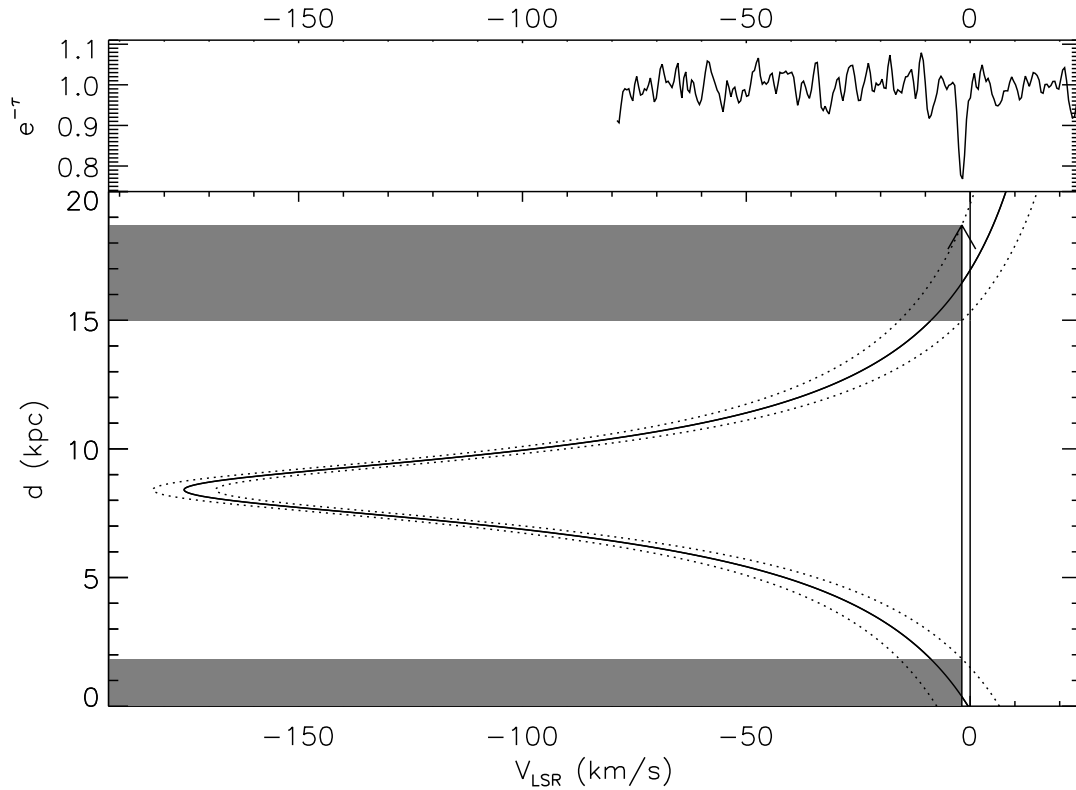


Fig. 3.— The velocity–distance relationship for the flat rotation curve of Fich et al. (1989). The 1667 MHz OH absorption line against PSR B1718-35 is shown in the top panel. The flat rotation curve is shown as the solid line in the lower panel. The dashed lines represent the random velocity of 7 km s^{-1} found for cold clouds (Lockman & Dickey 1990). The vertical arrow is at the center velocity of the OH absorption. The gray shaded areas show allowed distances for the OH absorption cloud. The distance is limited to be within 1.84 kpc of the Sun, given that PSR B1718-35 is on the near side of the tangent point (Weisberg et al. 1995).

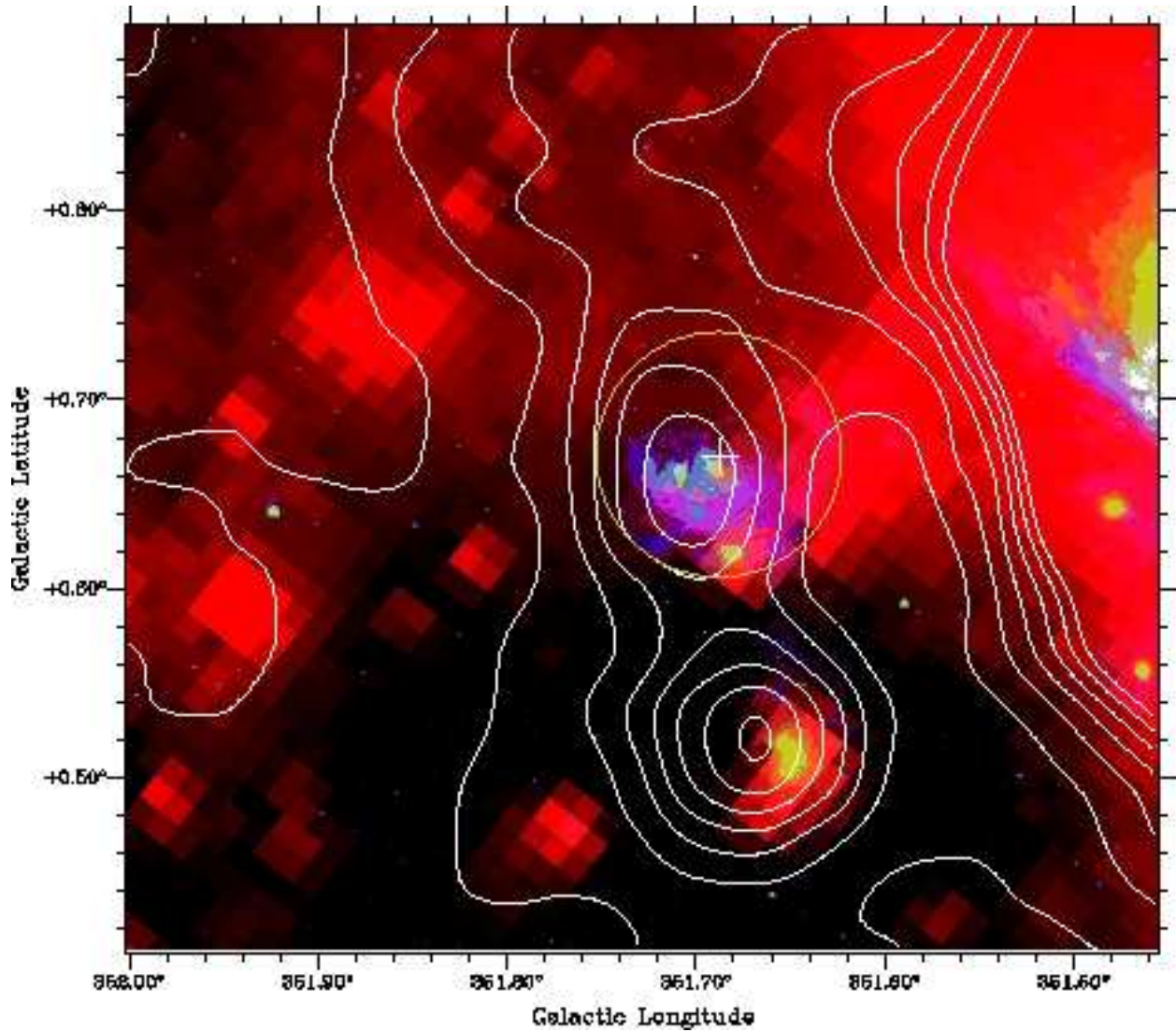


Fig. 4.— The region around PSR B1718-35. This false color image is comprised of Spitzer GLIMPSE II 8 micron data (blue), Spitzer MIPS 24 micron data (green), SHASSA H_α data (red) (Gaustad et al. 2001), and Parkes 6 cm continuum emission data (white contours) (Haynes et al. 1978). The contour levels are from 0 to 5 K every 0.5 K. The position of PSR B1718-35 is shown by the white cross. The size of the GBT beam at 1665 MHz is shown by the green circle. NGC 6334 is visible at the right edge of the image.

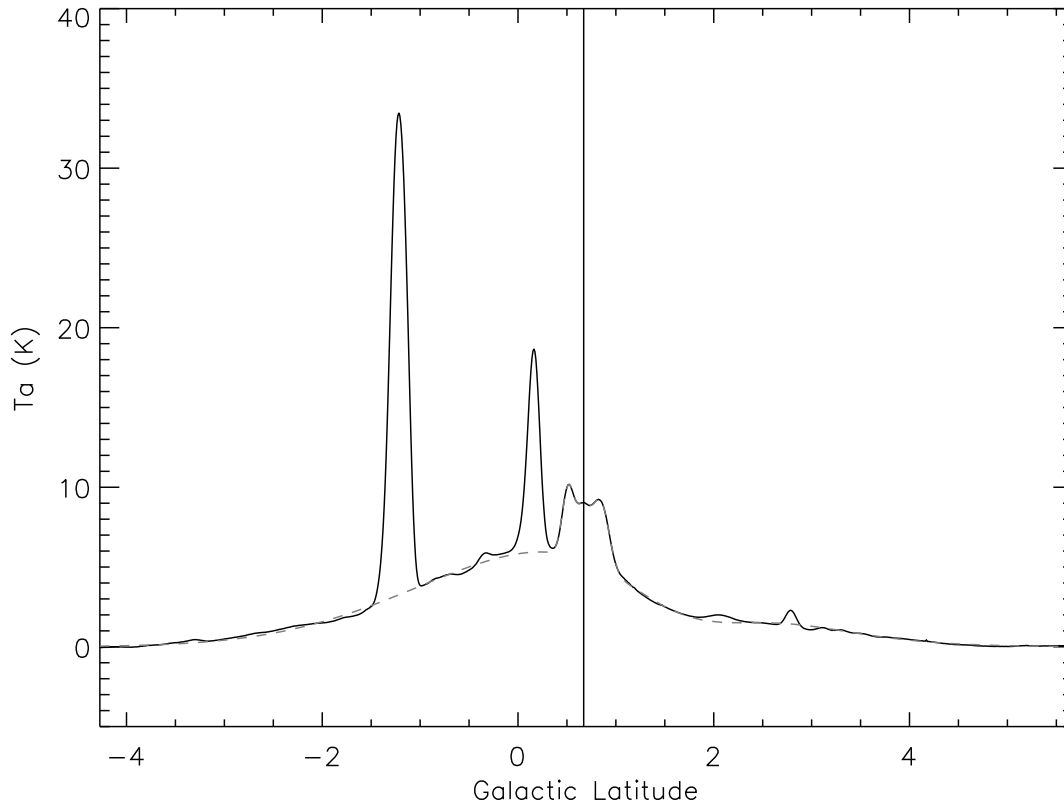


Fig. 5.— Continuum data slice along Galactic longitude $351^{\circ}688$ passing through the location of PSR B1718-35. These data have been corrected for atmospheric opacity ($\tau = 0.0103$, $T_{atm} = 250$ K) and have had a constant zenith system temperature of 15 K removed. The vertical line marks the position of PSR B1718-35. The dashed gray line is a two component Gaussian fit that can be assumed to approximate the smooth Galactic synchrotron and free-free emission contribution to the continuum emission along with three more Gaussians fitted for the continuum sources near the PSR B1718-35 line of sight. The total continuum emission toward PSR B1718-35 is 9.0 K. The smooth Galactic component is 5.8 K and the continuum source along the PSR B1718-35 line of sight is 2.9 K.

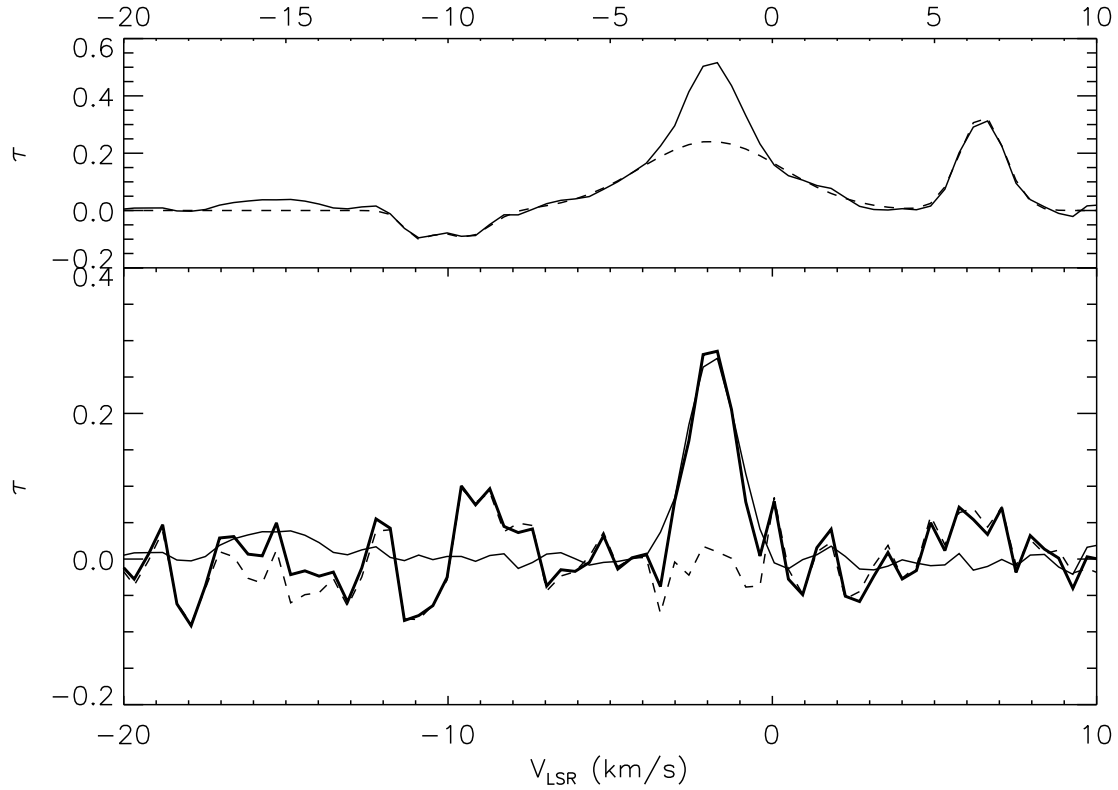


Fig. 6.— Top panel: The opacity of the pulsar 'off' 1665 MHz spectrum assuming a continuum flux of 2.1 K (solid line) and fitted Gaussians to the broad component of the absorption line seen against the pulsar and other lines (dashed line). Bottom Panel: Pulsar 1665 MHz opacity (thick solid line), the narrow component of the pulsar 'off' spectra after subtracting the fit to the broad component (thin solid line) and the differences between the spectra (dashed line).